

Investigation of Geothermal Systems in the Mount Meager Volcanic Complex, Southwestern British Columbia (Part of NTS 092J), Using 3-D Inversion of Audio-Magnetotelluric Data

F. Hormozzade Ghalati¹, Department of Earth Sciences, Carleton University, Ottawa, Ontario, fatemehormozzadeghal@cmail.carleton.ca

J.A. Craven, Natural Resources Canada, Geological Survey of Canada—Central, Ottawa, Ontario

D. Motazedian, Department of Earth Sciences, Carleton University, Ottawa, Ontario

S.E. Grasby, Natural Resources Canada, Geological Survey of Canada—Calgary, Calgary, Alberta

Hormozzade Ghalati, F., Craven, J.A., Motazedian, D. and Grasby, S.E. (2023): Investigation of geothermal systems in the Mount Meager Volcanic Complex, southwestern British Columbia (part of NTS 092J), using 3-D inversion of audio-magnetotelluric data; *in* Geoscience BC Summary of Activities 2022: Energy and Water, Geoscience BC, Report 2023-02, p. 55–62.

Introduction

Geothermal energy can provide reliable electricity and heat generation sources. Geothermal systems are geological settings defined by temperature, and geological and hydrological characteristics. In addition to heat and fluid source characteristics, reservoir properties such as porosity and permeability play an important role in determining whether a reservoir can be economically exploited for geothermal energy (Williams et al., 2011; Moeck, 2014).

Different geological, geochemical and geophysical techniques have been used to evaluate geothermal systems around the world. Geophysical exploration methods are required to image the fluid and temperature regimes of a geothermal system, as they provide a means of resolving reservoir physical parameters such as porosity and permeability (van Leeuwen et al., 2016). The fluid flow pathways in these reservoirs are often controlled by permeable and porous material created by geological features such as fractures, joints and faults. The objectives of these geophysical surveys are to define the boundary of a geothermal reservoir and its physical properties in order to evaluate its commercial viability (Didana et al., 2017; Thiel, 2017).

The magnetotelluric (MT) method is an electromagnetic exploration technique that measures the magnetic and electric fields on the Earth's surface (Chave and Jones, 2012). Natural electromagnetic waves span a broad frequency range of 0.001 to 40 000 Hz. The audio-magnetotelluric (AMT) method measures the natural electromagnetic fields at the higher frequencies (1 to 40 000 Hz), which permits mapping of shallow subsurface structures.

This project investigates the geothermal systems in the Mount Meager Volcanic Complex (MMVC) of southwestern British Columbia (BC) using 3-D inversion of AMT data. This project was initiated in 2019 in support of the geothermal research at the MMVC as part of the Garibaldi Geothermal Volcanic Belt Assessment Project (Grasby et al., 2020, 2021, 2023). This paper reviews the background of the AMT research and summarizes the results and the progress of ongoing research.

Study Area and Geological Setting

The MMVC, with elevations rising to >2600 m, is an active volcanic complex within the Garibaldi volcanic belt, situated approximately 150 km north of Vancouver, BC (Figure 1; Ghomshei and Clark, 1993; Jessop, 2008). The Garibaldi volcanic belt is a glaciovolcanic arc of young (<11 000 years old) volcanoes (e.g., Mount Garibaldi, Mount Cayley, Mount Meager [Wilson and Russell, 2018; Venugopal et al., 2020]), extending from the northern part of the State of Washington through southwestern BC (Figure 1; Jessop, 2008).

The geological units underlying the MMVC (including Mount Meager, Plinth Peak and Pylon Peak) are Mesozoic, fractured, crystalline and metamorphic rocks (Read, 1977). The volcanic rocks in the MMVC include basalt, andesite and rhyodacite flows, rhyodacite domes and pyroclastics (Read, 1977). The hydraulic conductivity of these basement rocks and volcanic rocks is mainly controlled by fracture porosity (Jamieson, 1981). In the MMVC, springs and vents trend northward and occur where rocks are fractured and dissected by faults (Bernard, 2020). Among these springs are the Meager Creek (30–59°C) and Placid (45°C) hot springs, and No Good warm spring (30–40°C), all of which lie along Meager Creek (Ghomshei and Clark, 1993; Proenza, 2012; Huang, 2019). Significant faults include the Meager Creek, No Good and Camp faults (Figure 2).

¹The lead author is a 2022 Geoscience BC Scholarship recipient.

This publication is also available, free of charge, as colour digital files in Adobe Acrobat® PDF format from the Geoscience BC website: <http://geosciencebc.com/updates/summary-of-activities/>.

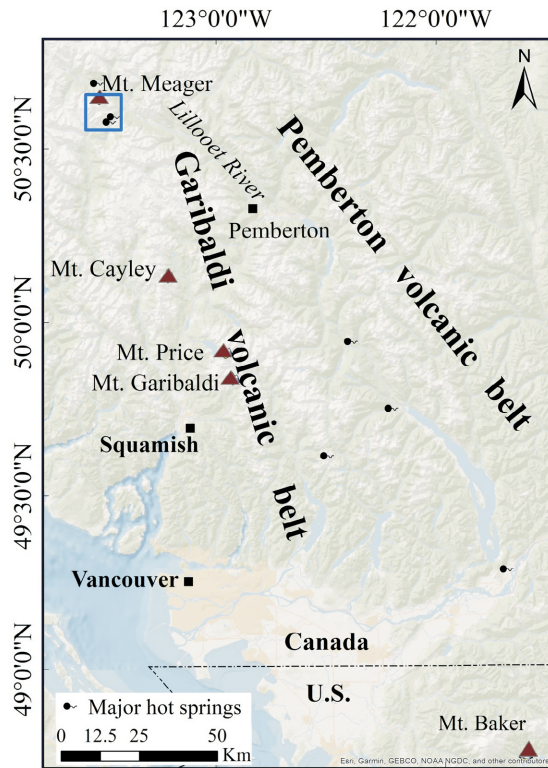


Figure 1. Location of the Garibaldi volcanic belt, southwestern British Columbia. Study area outlined in blue in northwestern corner (after Lewis et al., 1978; Hormozzade Ghalati et al., 2022).

Project Background

Research and exploration of geothermal resources at the MMVC, which has one of the highest geothermal potentials in Canada, have been conducted since the 1970s (Grasby et al., 2012). Previous MT surveys of the area used few stations and (now) outdated techniques (Jones and Dumas, 1993; Candy, 2001). By employing new techniques and equipment, a comprehensive AMT dataset (from 84 stations) was collected in 2019, and for the first time focused on the surface-to-reservoir depths to address the gaps of earlier studies (Figure 2; Craven et al., 2020; Hormozzade Ghalati et al., 2021a, b).

Data and Methodology

The MT method is a passive electromagnetic method that uses the Earth's natural electric (E) and magnetic (H) fields to identify subsurface electrical resistivity structures (Simpson and Bahr, 2005; Chave and Jones, 2012). In the MT method, an impedance tensor (Z) relates the E and H components in x and y directions (geographic coordinates), defining north and east, respectively, as

$$\begin{bmatrix} E_x \\ E_y \end{bmatrix} = \begin{bmatrix} Z_{xx} & Z_{xy} \\ Z_{yx} & Z_{yy} \end{bmatrix} \begin{bmatrix} H_x \\ H_y \end{bmatrix} \quad (1)$$

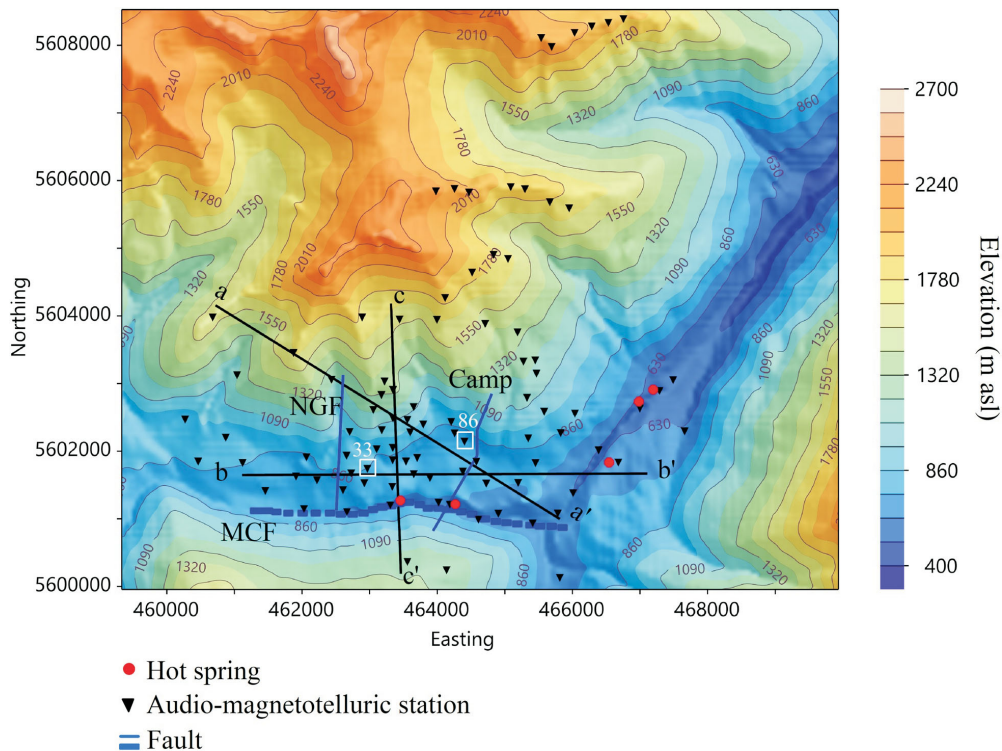


Figure 2. Overview of the study area, Mount Meager Volcanic Complex. Locations of stations in Figure 3 and cross-sections in Figure 5 are shown. All co-ordinates are in UTM Zone 10N, NAD 83. Abbreviations: Camp, Camp fault; MCF, Meager Creek fault; NGF, No Good fault.

Using inversion techniques, apparent resistivity (ρ_a) and the phase (Φ) are calculated (in i and j directions) from the impedance tensor's components, in imaginary (Im) and real (Re) parts, as functions of frequency (Equations 2, 3), depending on the angular frequency (ω) and the magnetic permeability of free space (μ_0 ; Simpson and Bahr, 2005).

$$\rho_{a,ij}(\omega) = \frac{1}{\omega\mu_0} [Z_{ij}(\omega)]^2 \quad (2)$$

$$\Phi_{ij}(\omega) = \tan^{-1} \left(\frac{\text{Im}(Z_{ij}(\omega))}{\text{Re}(Z_{ij}(\omega))} \right) \quad (3)$$

Producing an electrical resistivity model from inversion of MT data provides a tool for estimating the physical properties of rocks. The electrical resistivity of rocks is influenced by factors such as lithology, porosity, temperature and salinity of the fluid filling the pores (Chave and Jones, 2012). Also, fault and fracture zones that contribute to fluid circulation may exhibit electrical resistivity differences (Muñoz, 2014). Rocks have different mineral contents with variable pore shapes and interconnectivity, all of which can influence the electrical resistivity ($\rho=1/\sigma$ where σ is electrical conductivity), defined by Archie's law (Archie, 1942):

$$\sigma_f = \sigma_b \phi^{-m}, \quad (4)$$

where ϕ is porosity, m is the cementation factor, σ_b is the bulk electrical conductivity and σ_f is the fluid electrical conductivity (Siemens/metre [S/m]). A modified Archie's law defines the relationship between electrical conductivity and porosity considering two-phased electrical conductivity (σ_s is the solid phase conductivity of the material [S/m]; Glover et al., 2000):

$$\sigma_b = \sigma_f \phi^m + \sigma_s (1-\phi)^p \quad (5)$$

$$p = \frac{\log(1-\phi^m)}{\log(1-\phi)}$$

Results

This paper presents an overview of the project's preliminary results and the ongoing research direction. Detailed results of the 3-D inversion of the AMT data can be found in Hormozzade Ghalati et al. (2022).

The preferred electrical resistivity model is based on CCG's RLM3D MT inversion code, used to invert the impedance tensors (Soyer et al., 2020). The model was discretized into 153 by 116 by 89 cells in three dimensions, northwest-southeast, northeast-southwest and depth, respectively. The central core of the model mesh was divided into 75 by 75 m cells for lateral discretization. Padding was added around the core area for boundary condition calculations. The dimensions of these paddings were calculated

using a multiplicative factor of 1.5 in all lateral directions. Layers in the MT model were discretized into 40 m thicknesses at elevations of 475–2350 m above sea level (asl), to give high accuracy responses for the data on the mountainsides. Subsequent layers were increased by a factor of 1.12 to a depth of 3500 m below sea level (bsl), and a factor of 1.25 to the bottom of the model. The overall root mean square (RMS) of the inversion was 1.30 after 75 iterations. The apparent resistivity and phase responses of the 3-D inversion model fit well to the observed data. Comparison between the observed data and the calculated responses for two stations (33 and 86) were plotted to assess the data misfit at the final iteration (Figure 3a, b).

The resistivity model normally identifies values above 200 ohm-m ($\Omega\cdot\text{m}$) that are immediately under the surface, which can be interpreted as a region (R) where hot geothermal fluids do not alter the rocks and the temperature is less than 70°C. The section beneath this layer is a conductive zone. At MMVC, two conductive zones (C1, C2) were correlated with the location of faults, distribution of alteration minerals, as reported in borehole geological logs, and measured temperatures (Figures 4, 5a–c). Conductive zone C1 reaches the surface where hot and warm springs seep into Meager Creek and is well correlated with the location of springs (Figure 5b, c). In boreholes, these shallower zones (C1, C2) can be correlated to argillic alteration minerals, characterized by the presence of smectite, illite and rare kaolinite, and measured temperatures of 70–160°C (Proenza, 2012, and references contained therein). The C1 and C2 conductive zones observed in the model are interpreted to map the low permeability clay-rich layers that act as caprocks and enable the accumulation of deeper hot fluids. The caprock is located on top of a zone with higher resistivity values (15–150 $\Omega\cdot\text{m}$), corresponding to borehole temperatures of 160–270°C (Figure 5a; Proenza, 2012, and references contained therein).

The results show the potential of using 3-D inversion of AMT data to map the fluid pathways at MMVC. These pathways are moderately conductive zones that show high porosity using Archie's law and modified Archie's law (Equations 4, 5). Moreover, these pathways correlate with lost-circulation zones in borehole logs (Proenza, 2012, and references contained therein).

Summary and Future Work

This project provides a detailed near-surface electrical resistivity model of the Mount Meager Volcanic Complex (MMVC) study area, using data from a dense grid of audio-magnetotelluric (AMT) stations, and a modern algorithm, which allowed 3-D mapping of the reservoir zones that accounted for the steep mountain topography. The resistivity model demonstrates the pattern of caprock and fluid flow zones in the area. Geological log and temperature data were

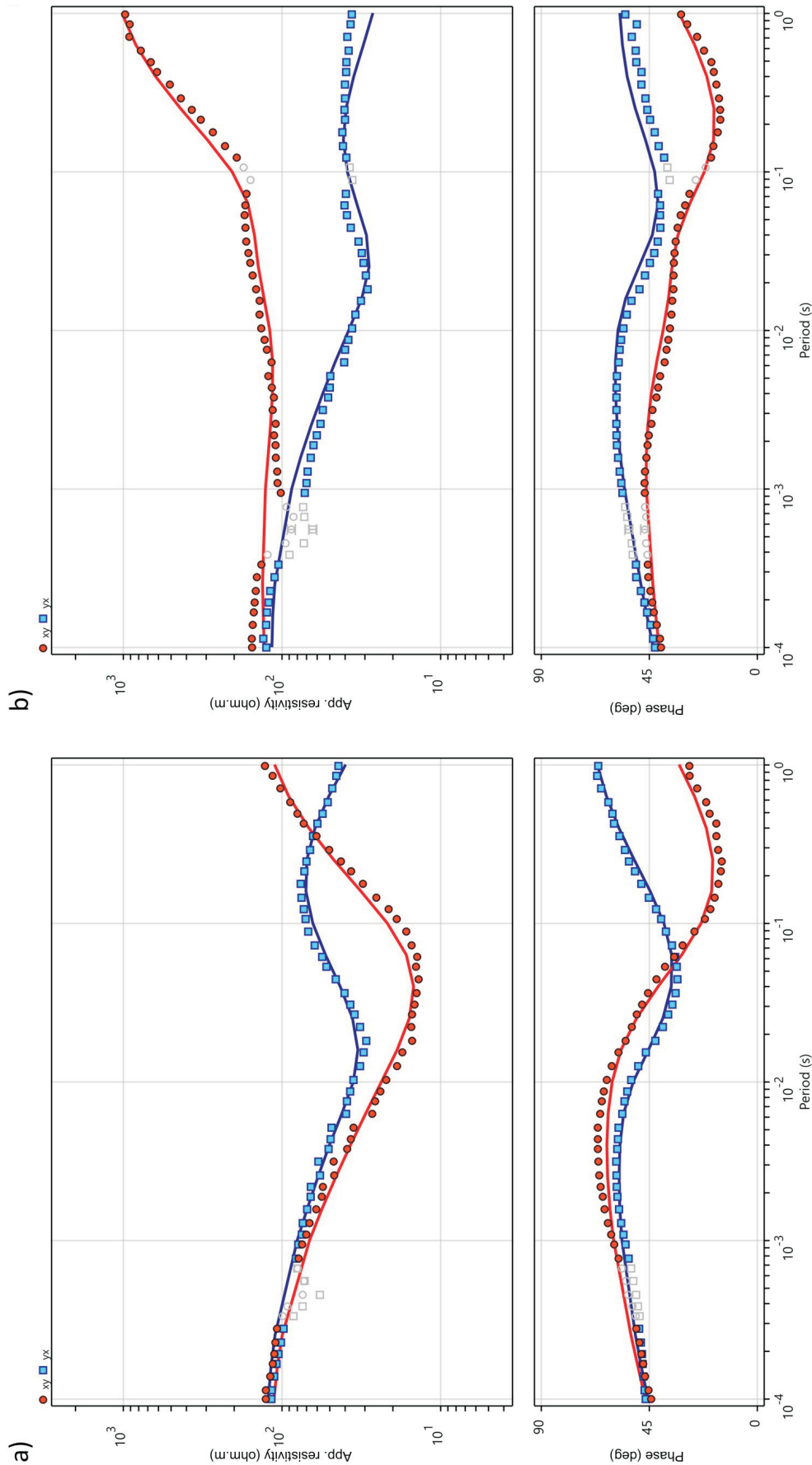


Figure 3. Fit of the observed and estimated apparent (App.) resistivity and phase of the preferred 3-D inversion model for **a)** station 33 and **b)** station 86, Mount Meager Volcanic Complex study area (see Figure 2 for station locations). The observed values of xy and yx components are represented by red circles and blue squares and the estimated xy and yx components are shown by red and blue lines, respectively. Masked data are shown in grey. Abbreviation: deg, degrees.

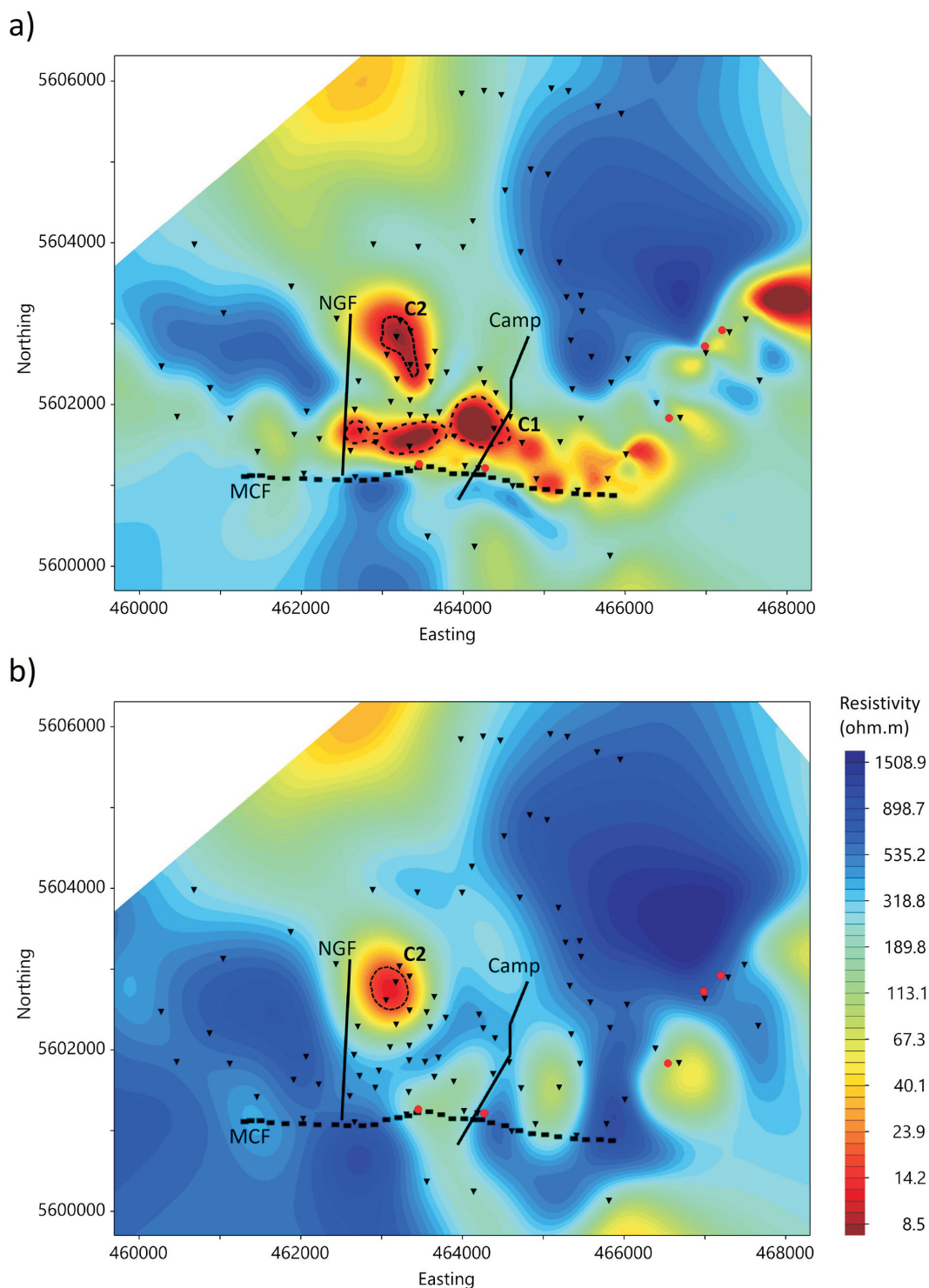
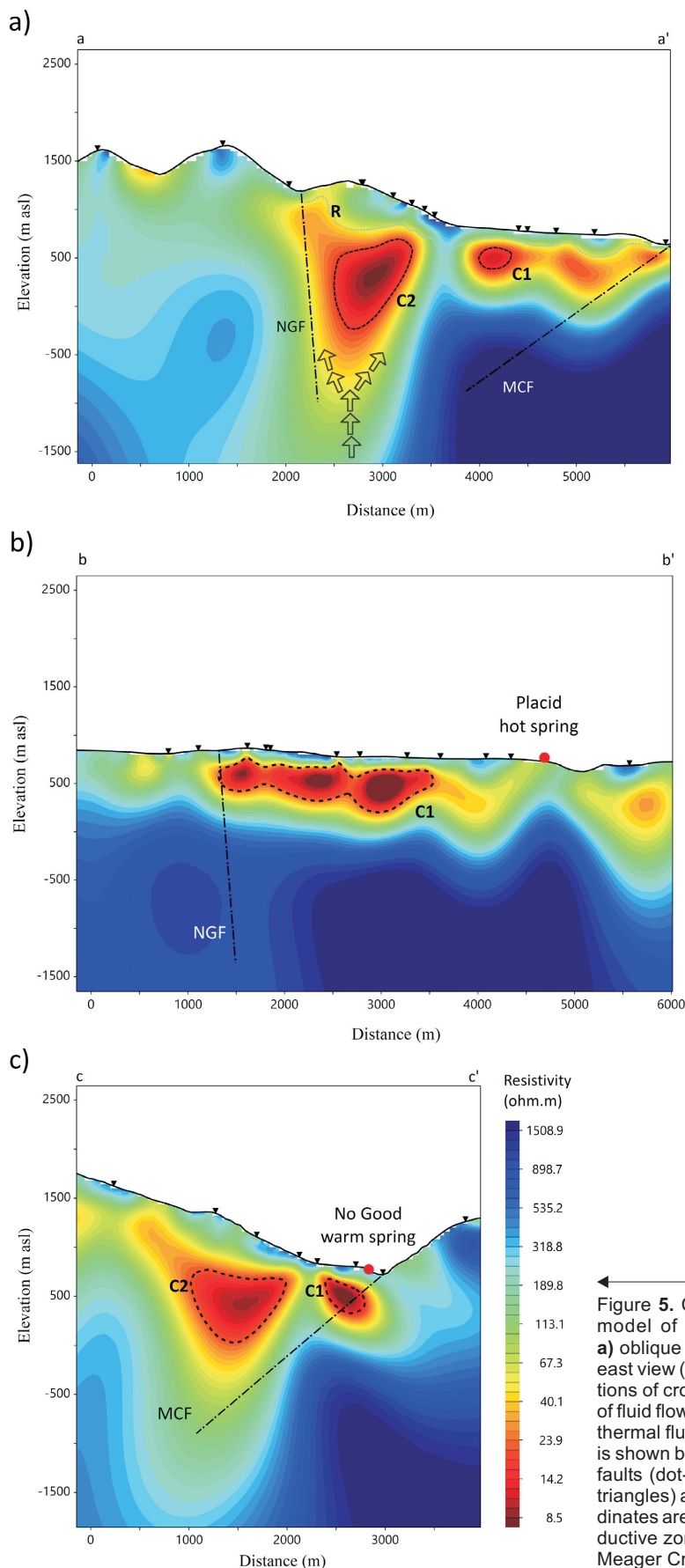


Figure 4. Horizontal plan views from the final audio-magnetotelluric model at elevations of **a)** 500 m above sea level (m asl), and **b)** 0 m asl, at the Mount Meager Volcanic Complex study area. Location of hot springs (red dots), faults (solid and dashed lines) and audio-magnetotelluric stations (black triangles) are shown. Colour bar is the same for both plots. All co-ordinates are in UTM Zone 10N, NAD 83. Abbreviations: C1, C1 conductive zone; C2, C2 conductive zone; Camp, Camp fault; MCF, Meager Creek fault; NGF, No Good fault.



integrated into the resistivity model. A possible interpretation for the conductive zones is that they are impermeable caprocks that act as the seal for underlying geothermal reservoirs. The caprock is interpreted to be deeper in the northern part of the study area, which can be considered for exploitation purposes. Since clay minerals do not have sufficient effective porosity and permeability to permit fluid flow to the production wells, considering such models reduces the risk of future development of geothermal resources.

As this is an ongoing project, further studies are needed to evaluate the petrophysical properties of the geothermal reservoirs. Future work is planned to 1) include laboratory measurements and rock physical properties to estimate reservoir characteristics based on the AMT electrical resistivity model of the MMVC study area and 2) incorporate a previously published deep MT model to find the relationship between shallow conductors, magma source and possible fluid pathways at the MMVC study area.

The MMVC was selected for the current study due to a wealth of legacy data, a result of its role as the first target for geothermal exploration in Canada. This area has potential due to the existence of warm and hot springs, extensive borehole coverage and nearby communities supportive of alternative energy development. Results of this project will improve the understanding of the geology and hydrothermal alteration caused by circulating hot water and provide insight into ideal locations for further production and reinjection boreholes. The results and the continuation of this research will support the broader goals of reducing the technical and economic risks of geothermal exploration in the Garibaldi volcanic belt.

Figure 5. Cross-sectional views through the final 3-D resistivity model of the Mount Meager Volcanic Complex study area: **a)** oblique view in northwest-southeast direction (a–a'), **b)** west-east view (b–b'), **c)** north-south view (c–c'). See Figure 2 for locations of cross-sections. Black arrows show the potential direction of fluid flow. The limit of the near surface region (R) where hot geothermal fluids do not alter the rocks and the temperature is <70°C is shown by a dashed blue line. Location of hot springs (red dots), faults (dot-dash lines) and audio-magnetotelluric stations (black triangles) are shown. Colour bar is the same for all plots. All co-ordinates are in UTM Zone 10N, NAD 83. Abbreviations: C1, C1 conductive zone; C2, C2 conductive zone; Camp, Camp fault; MCF, Meager Creek fault; NGF, No Good fault.

Acknowledgments

This project was funded by Natural Resources Canada and Geoscience BC and benefited from support of the Natural Sciences and Engineering Research Council of Canada through Carleton University. The authors would like to thank W. Yuan for reviewing this manuscript. The authors would like to thank E. Roots for providing his pyMT program, V. Tschirhart, R. Bryant, S.M. Ansari and J. Liu for helping during the field survey, T. Jenkins from the Lil'wat First Nation for ensuring wildlife were undisturbed, M. Accurso, D. Vincent and R. Slinger for piloting (No Limits Helicopters), and Innergex Renewable Energy Inc. for providing significant access to their field bunkhouse.

References

- Archie, G.E. (1942): The electrical resistivity log as an aid in determining some reservoir characteristics; *Transactions of the AIME*, v. 146, no. 1, p. 54–62, URL <<https://doi.org/10.2118/942054-G>>.
- Bernard, K. (2020): Epithermal clast coating inside the rock avalanche-debris flow deposits from Mount Meager Volcanic Complex, British Columbia (Canada); *Journal of Volcanology and Geothermal Research*, v. 402, art. 1069994, URL <<https://doi.org/10.1016/j.jvolgeores.2020.106994>>.
- Candy, C. (2001): Crew development corporation report on a magnetotelluric survey, South Meager geothermal project, Pemberton, British Columbia; Frontier Geosciences Inc., unpublished report for Frontier Geosciences project FG1-581.
- Chave, A.D. and Jones, A.G. (2012): *The Magnetotelluric Method: Theory and Practice*; Cambridge University Press, New York, New York, 552 p.
- Craven, J.A., Hormozzade, F., Tschirhart, V., Ansari, M., Bryant, R. and Montezadian, D. (2020): Overview of the 2019 audiomagnetotelluric survey of the Mount Meager geothermal reservoir; Chapter 6 in *Garibaldi Geothermal Energy Project, Mount Meager 2019 - Field Report*, Geoscience BC, Report 2020-09, p. 126–147, URL <https://www.geosciencebc.com/i/project_data/GBCReport2020-09/GeoscienceBCReport%202020-09.pdf> [March 2021].
- Didana, Y.L., Heinson, G., Thiel, S. and Krieger, L. (2017): Magnetotelluric monitoring of permeability enhancement at enhanced geothermal system project; *Geothermics*, v. 66, p. 23–38, <<https://doi.org/10.1016/j.geothermics.2016.11.005>>.
- Ghomshei, M.M. and Clark, I.D. (1993): Oxygen and hydrogen isotopes in deep thermal waters from the south Meager Creek geothermal area, British Columbia, Canada; *Geothermics*, v. 22, no. 2, p. 79–89, URL <[https://doi.org/10.1016/0375-6505\(93\)90048-R](https://doi.org/10.1016/0375-6505(93)90048-R)>.
- Glover, P.W.J., Hole, M.J. and Pous, J. (2000): A modified Archie's law for two conducting phases; *Earth and Planetary Science Letters*, v. 180, no. 3–4, p. 369–383, URL <<https://www.sciencedirect.com/science/article/pii/S0012821X00001680>> [May 2022].
- Grasby, S.E., Allen, D.M., Bell, S., Chen, Z., Ferguson, G., Jessop, A., Kelman, M., Ko, M., Majorowicz, J., Moore, M., Raymond, J. and Therrien, R. (2012): Geothermal energy resource potential of Canada; Geological Survey of Canada, Open File 6914, 322 p., URL <<https://doi.org/10.4095/291488>>.
- Grasby, S.E., Ansari, S.M., Barendregt, R.W., Borch, A., Calahorrano-DiPatre, A., Chen, Z., Craven, J.A., Dettmer, J., Gilbert, H., Hannenson, C., Harris, M., Hormozzade, F., Leiter, S., Liu, J., Muhammad, M., Quane, S.L., Russell, J.K., Salvage, R.O., Savard, G., Tschirhart, V. et al. (2021): Garibaldi Geothermal Energy Project – phase 1 – final report; Geoscience BC, Report 2021–08, 276 p., URL <https://www.geosciencebc.com/i/project_data/GBCReport2021-08/GBCR%202021-08%20Garibaldi%20Geothermal%20Energy%20Project%20-%20Phase%201.pdf> [February 2022].
- Grasby, S.E., Ansari, S.M., Calahorrano-DiPatre, A., Chen, Z., Craven, J.A., Dettmer, J., Gilbert, H., Hannenson, C., Harris, M., Liu, J., Muhammad, M., Russell, K., Salvage, R.O., Savard, G., Tschirhart, V., Unsworth, M.J., Vigouroux-Caillibot, N. and Williams-Jones, G. (2020): Geothermal resource potential of the Garibaldi volcanic belt, southwestern British Columbia (part of NTS 092J); in *Geoscience BC Summary of Activities 2019: Energy and Water*, Geoscience BC, Report 2020-02, p. 103–108, URL <https://www.geosciencebc.com/i/pdf/SummaryofActivities2019/EW/Project%202018-004_EW_SOA2019.pdf> [February 2022].
- Grasby, S.E., Borch, A., Calahorrano-DiPatre, A., Chen, Z., Craven, J., Liu, X., Muhammad, M., Russell, J.K., Tschirhart, V., Unsworth, M.J., Williams-Jones, G. and Yuan, W. (2023): Garibaldi Geothermal Volcanic Belt Assessment Project, southwestern British Columbia (part of NTS 092J) phase 2: 2022 field report; in *Geoscience BC Summary of Activities 2022: Energy and Water*, Geoscience BC, Report 2023-02, p. 47–54, URL <<https://geosciencebc.com/updates/summary-of-activities>>.
- Hormozzade Ghalati, F., Craven, J.A., Motazedian, D., Grasby, S.E. and Roots, E. (2021a): Shallow geothermal reservoir exploration in Mt. Meager, British Columbia, Canada; American Geophysical Union, AGU Fall Meeting, December 13–17, 2021, New Orleans, Louisiana, abstract, URL <<https://ui.adsabs.harvard.edu/abs/2021AGUFMGP21A..10H/abstract>> [December 2021].
- Hormozzade Ghalati, F., Craven, J.A., Motazedian, D., Grasby, S.E., Roots, E., Tschirhart, V., Ansari, S.M. and Liu, J. (2021b): Exploring the near surface geothermal structure at Mt. Meager, British Columbia, Canada; European Geosciences Union, EGU General Assembly Conference, April 19–30, 2021, virtual, abstract EGU21-12542, URL <<https://doi.org/10.5194/egusphere-egu21-12542>>.
- Hormozzade Ghalati, F., Craven, J.A., Motazedian, D., Grasby, S.E. and Tschirhart, V. (2022): Modeling a fractured geothermal reservoir using 3-D AMT data inversion: insights from Garibaldi volcanic belt, British Columbia, Canada; *Geothermics*, v. 105, art. 102528, URL <<https://doi.org/10.1016/j.geothermics.2022.102528>>.
- Huang, K. (2019): Geochemical analysis of thermal fluids from southern Mount Meager, British Columbia, Canada; M.Sc. thesis, University of Iceland, 92 p., URL <<https://skemman.is/bitstream/1946/33384/1/Katherine%20Huang%20MS%20Thesis.pdf>> [September 2021].
- Jamieson, G.R. (1981): A preliminary study of the regional groundwater flow in the Meager Mountain geothermal area, British Columbia; M.Sc. thesis, The University of British Columbia, 163 p., URL <<http://hdl.handle.net/2429/22494>> [May 2020].

- Jessop, A. (2008): Review of National Geothermal Energy Program, Phase 2 – geothermal potential of the Cordillera; Geological Survey of Canada, Open File 5906, 86 p., URL <<https://doi.org/10.4095/225917>>.
- Jones, A.G. and Dumas, I. (1993): Electromagnetic images of a volcanic zone; *Physics of the Earth and Planetary Interiors*, v. 81, p. 289–314, URL <[https://doi.org/10.1016/0031-9201\(93\)90137-X](https://doi.org/10.1016/0031-9201(93)90137-X)>.
- Lewis, T.J., Judge, A.S. and Souther, J.G. (1978): Possible geothermal resources in the Coast Plutonic Complex of southern British Columbia, Canada; *Pure and Applied Geophysics*, v. 117, no. 1, p. 172–179, URL <<https://doi.org/10.1007/BF00879744>>.
- Moeck, I.S. (2014): Catalog of geothermal play types based on geologic controls; *Renewable and Sustainable Energy Reviews*, v. 37, p. 867–882, URL <<https://doi.org/10.1016/j.rser.2014.05.032>>.
- Muñoz, G. (2014): Exploring for geothermal resources with electromagnetic methods; *Surveys in Geophysics*, v. 35, p. 101–122, URL <<https://doi.org/10.1007/s10712-013-9236-0>>.
- Proenza, Y. (2012): Geothermal data compilation and analysis of Alterra Power’s upper Lillooet property; M.Eng. thesis, The University of British Columbia, 47 p., URL <https://www.geosciencebc.com/i/project_data/GBC2017-006/Yuliana%20Proenza%20MEng%20Project.zip> [September 2019].
- Read, P.B. (1977): Meager Creek volcanic complex, southwestern British Columbia; *in* Report of Activities, Part A, Geological Survey of Canada, Paper no. 77-1A, p. 277–281.
- Simpson, F. and Bahr, K. (2005): *Practical Magnetotellurics*; Cambridge University Press, Cambridge, United Kingdom, 270 p., URL <<https://doi.org/10.1017/CBO9780511614095>>.
- Soyer, W., Mackie, R., Miorelli, F., Schifano, V. and Hallinan, S. (2020): 3D inversion modeling of natural and controlled source EM in complex terrain; European Association of Geoscientists & Engineers, NSG2020 3rd Conference on Geophysics for Mineral Exploration and Mining, December 7, 2020, virtual, v. 2020, p. 1–4, URL <<https://doi.org/10.3997/2214-4609.202020208>>.
- Thiel, S. (2017): Electromagnetic monitoring of hydraulic fracturing: relationship to permeability, seismicity, and stress; *Surveys in Geophysics*, v. 38, no. 5, p. 1133–1169, URL <<https://doi.org/10.1007/s10712-017-9426-2>>.
- van Leeuwen, W.A. (2016): Geothermal exploration using the magnetotelluric method; Ph.D. thesis, Utrecht University, 277 p., URL <<https://dspace.library.uu.nl/bitstream/handle/1874/340000/vLeeuwen.pdf?sequence=1&isAllowed=y>> [November 2022].
- Venugopal, S., Moune, S., Williams-Jones, G., Druitt, T., Vigouroux, N., Wilson, A. and Russell, J.K. (2020): Two distinct mantle sources beneath the Garibaldi volcanic belt: insight from olivine-hosted melt inclusions; *Chemical Geology*, v. 532, art. 119346, URL <<https://doi.org/10.1016/j.chemgeo.2019.119346>>.
- Williams, C.F., Reed, M.J. and Anderson, A.F. (2011): Updating the classification of geothermal resources; *in* Proceedings, 36th Workshop on Geothermal Reservoir Engineering, Stanford University, January 31–February 2, 2011, Stanford, California, URL <<http://pangea.stanford.edu/ERE/pdf/IGAstandard/SGW/2011/williams.pdf>> [February 2022].
- Wilson, A.M. and Russell, J.K. (2018): Quaternary glaciovolcanism in the Canadian Cascade volcanic arc – paleoenvironmental implications; *in* Field Volcanology: A Tribute to the Distinguished Career of Don Swanson, M.P. Poland, M.O. Garcia, V.E. Camp and A. Grunder (ed.), Geological Society of America, Special Paper 538, p. 133–157, URL <[https://doi.org/10.1130/2018.2538\(06\)](https://doi.org/10.1130/2018.2538(06))>.